

Effects of the 9T Magnetic Field on MRS Photodiode

D. Beznosko^a, G. Blazey, A. Dyshkant, V. Rykalin

Northern Illinois University, Dekalb, IL 60115 USA

Abstract

The experimental results on the performance of the MRS (Metal/Resistor/Semiconductor) photodiode in the strong magnetic field of 9T, and the possible impact of the quench of the magnet at 9.5T on sensor's operation are reported. The measurement method used is being described. The results of the work agree with the expectations that the MRS photodiode is not exhibiting sensitivity to the magnetic field presence. This result is essential for the design of the future electron-positron linear collider detector.

PACS-1996 codes: 29.40.Wk, 29.40.Mc, 29.40.Vj

Keywords: solid-state photosensor, UV LED, magnetic field, scintillator, extruded, effects

^a Corresponding Author: Dmitriy Beznosko, 4107 47ave #3D, Sunnyside, NY 11104 USA (telephone: 347-992-6486, email: dima@dozory.org).

I. INTRODUCTION

Future detectors (like Hadron Calorimeter [1] [2] for a future e+e- linear collider) may require the use of scintillator-based elements (i.e. cells) with embedded photodetectors, immersed in a strong magnetic field, or in tail catcher and muon tracker that are not in the field itself but they are influenced by the scattered fields. The performance requirement of photodetectors in the magnetic field has directed our attention to the latest developments of solid-state photomultipliers working in avalanche mode [3]. In this paper we have concentrated on the possible issues of the MRS output in the presence of strong magnetic field: i.e., the dependence of output's amplitude, area and rise time on the field, and the possible damaging effects of magnet's quench on the sensor. This paper shows the improved measurements conducted at 9T, with similar measurements carried out at lower fields (4.4T) earlier [4].

II. DESCRIPTIONS AND SCHEMATICS

A. *MRS Photodiode Description and Operational Principle*

The MRS photodiode is a multi-pixel solid-state device with every pixel operating in the limited Geiger multiplication mode. A resistive layer on the sensor's surface accomplishes avalanche quenching. The devices tested were of round shape, and they had ~ 1000 pixels per 1.1mm diameter photosensitive area, with the quantum efficiency (QE) of the device reaching $\sim 25\%$ at 500nm [5]. Due to the fact that the thickness of the active layer of this sensor is about 7 microns, MRS is theoretically expected to be non-sensitive to the magnetic field.

B. *Magnet Description*

All magnetic field measurements were performed at the Fermilab Magnet Test Facility. The magnet used for MRS measurements only was a new superconducting magnet with 29mm aperture and field up to 10T at about 2°K, which currently is under the test at Fermilab. The sensors were placed in the body of the magnet (far from the ends) to achieve field uniformity. The temperature in the magnet aperture was not cryogenic and was closer to room temperature, around 5-6°C.

C. MRS Module Description

For this test, five MRS sensors were used, arranged in different directions with respect to the magnetic field. All sensors were biased at 29.1V and 30.0V that were well within operating range of all five. An optical splitter was used to deliver similar amounts of light in the same pulse to each of the sensors.

The crystal used for splitting the light had a square cross-section being 5mm wide and 30mm long. At the output (front) end it had five symmetrical conical holes with 2mm base diameter for each of them (Fig. 1a). The conical surfaces were not polished. Without these conical holes, the ratio of the direct light along the crystal to the “side” light at the front end the crystal was about 10 to 1. With the conical holes, this ratio was less than two. No further effort was made to achieve the same amount of light in all directions since the goal was to get a comparable amount of light only. The positions of the photodetectors around the crystal were determined by these holes. The light splitting property of the crystal as measured by the same sensor is presented in Fig. 1b. Table I shows the various properties of MRS output for all 5 sensors in their places with the test signal applied in the absence of magnetic field.

The light pulse was produced by the Bivar [6] UV LED (peak emission ~400nm). The pulse from the pulse generator was ~30ns wide with ~5.5V amplitude. The LED was embedded into the 10mm thick extruded scintillator [7]. The LED-scintillator part was placed well outside the magnet to avoid any effects of the field on it since only the photodetectors were studied here. The light pulse from the scintillator to the splitter was carried via ~2.5m long, 2mm outer diameter, KURARAY [8], multicladd, Y-11, wavelength shifting (WLS) fiber. The outputs of the sensors were fed into the Agilent [9] Infiniium 54832D MSO oscilloscope without additional preamplifier. The schematic of this module is given in Fig. 2a, and the schematic of the power circuit for the MRS is drawn in Fig. 2b. The temperature inside the magnet was measured before and after the tests and was $5.0^{\circ}\text{C} \pm 0.5$.

III. MRS EXPERIMENTAL RESULTS

The data for all 5 channels were obtained. Because of the similarity of the results, data only for channel 4 will be presented for illustrative purposes. This channel corresponds to the MRS sensor that was positioned at the tip of the

splitter. The electrons in this sensor move along the same axis inside the magnet as the particle beam would, therefore, the MRS in channel 4 should experience the biggest effects of the B field, if any.

The following characteristics of the sensor's output were measured: amplitude, area, and rise time. Measurements were carried out at 0T, 5T, 9T at 29.1V bias, and at 0T and 9T for 30.0V bias. In addition, measurements were performed immediately after magnet quench at 9.5T (the field was already zero during these measurements). The pole with the sensors and the LED-scintillator part was inserted into the magnet approximately 4 hours before the experiment so that it would be at the same temperature as inside the dipole. A constant stream of nitrogen was pumped through the magnet throughout the test to remove the humidity.

Fig. 3 shows the values of the area of MRS output as a function of the magnetic field strength. The area is a measure of total charge of the output with a 50Ω load. Each point in every figure is an average of at least few hundred measurements at each field strength value. The errors are given directly by the oscilloscope. Here and in all further plots 9.5qT label indicates a measurement done after the magnet quench at 9.5T field, and 0T3 and 9T3 labels indicate measurements done at 30.0V bias. The biggest difference between points at 0T and 9T is ~2% that is within the measurement error.

Fig. 4 shows the values of the amplitude of MRS output as a function of the magnetic field strength. The amplitude is a measure of the peak current of the output with a 50Ω load. The maximum of ~1.5% change in output amplitude between field strength values of 0T and 9T is observed.

The dependence of rise time on the magnetic field strength was also studied (Fig. 5). The behavior of the signal rise time seems to be quite independent on the field strength with The maximum of ~1.5% change in output amplitude between field strength values of 0T and 9T is observed.

IV. CONCLUSIONS

Measurements performed using five MRS sensors in the strong magnetic field point to the insensitivity of the sensors outputs to the field strength of up to 9T within 1.5%-2%. In addition, measurements of the magnet quench

effects on the MRS sensor indicate that magnet quench did not damage the sensors, and had none or immeasurably small lasting effect on the sensors outputs.

Overall, the results agree with the expectations and are essential to using MRS photosensor in the calorimeter for the future international e^+e^- linear collider that is fully immersed in the magnetic field, or any other detector parts like tail-catcher or muon tracker that feel effects of scattered magnetic field.

V. ACKNOWLEDGMENT

The authors would like to thank Michael Tartaglia and the Fermilab Magnet Test Facility staff for useful advices, help, and patience that made this test possible.

VI. REFERENCES

- [1] A. Dyshkant, D. Beznosko, G. Blazey, D. Chakraborty, K. Francis, D. Kubik et al., "Towards a Scintillator-Based Digital Hadron Calorimeter for the Linear Collider Detector", IEEE vol. 51, no. 4, pp.1590-1595, Aug. 2004.
- [2] A. Dyshkant, D. Beznosko, G. Blazey, D. Chakraborty, K. Frances, D. Kubik et al, "Small Scintillating Cells as the Active Elements in a Digital Hadron Calorimeter for the e+e- Linear Collider Detector", FERMILAB-PUB-04/015, Feb 9, 2004
- [3] D. Beznosko, G. Blazey, D. Chakraborty, A. Dyshkant, K. Francis, D. Kubik et al., "Investigation of a Solid State Photodetector", NIM A, Volume 545, Issue 3, 21 June 2005, Pages 727-737.
- [4] D. Beznosko, G. Blazey, A. Dyshkant, V. Rykalin, V. Zutshi, "MRS Photodiode, LED and Extruded Scintillator in Magnetic Field", FERMILAB-PUB-05-122, May 09 2005
- [5] M. Golovin, A. V. Akindinov, E. A. Grigorev, A. N. Martemyanov, P.A. Polozov, "New Results on MRS APDS", Nucl. Instrum. Meth. A387 231-234, 1997
- [6] Bivar Inc., 4 Thomas, Irvine, CA 92618, USA
- [7] D. Beznosko, A. Bross, A. Dyshkant, A. Pla-Dalmau V. Rykalin, "FNAL-NICADD Extruded Scintillator", FERMILAB-CONF-04-216-E, September 15, 04
- [8] Kuraray America Inc., 200 Park Ave, NY 10166,USA; 3-1-6, NIHONBASHI, CHUO-KU, TOKYO 103-8254, JAPAN.
- [9] Agilent Technologies, Inc. Headquarters, 395 Page Mill Rd., Palo Alto, CA 94306, United States

TABLE I
OUTPUTS FOR 5 CHANNELS WITH TEST SIGNAL

Channel #	1	2	3	4	5
Area (nVs)	15.24	23.12	10.75	25.59	13.51
Amplitude (mV)	38.79	45.86	27.18	50.6	38.31
Rise time (ns)	30.55	43.16	33.69	38.94	30.50

Figure Captions:

Fig. 1a. Schematic of the splitting crystal (cross section along the splitter).

Fig. 1b. Uniformity of light output of splitting crystal.

Fig. 2a. MRS module schematics.

Fig. 2b. MRS power circuit schematics.

Fig. 3. Area of the MRS output.

Fig. 4. Amplitude of the MRS output.

Fig. 5. Rise time of the MRS output.

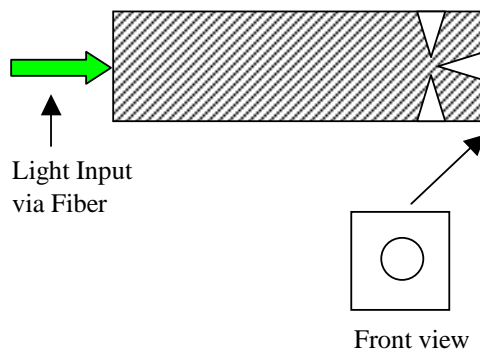


Fig. 1a.

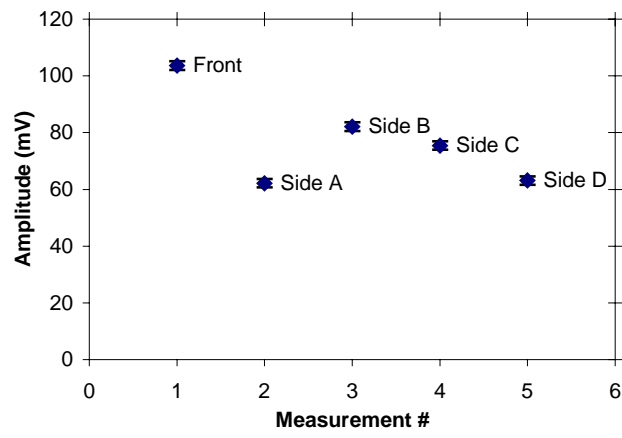


Fig. 1b.

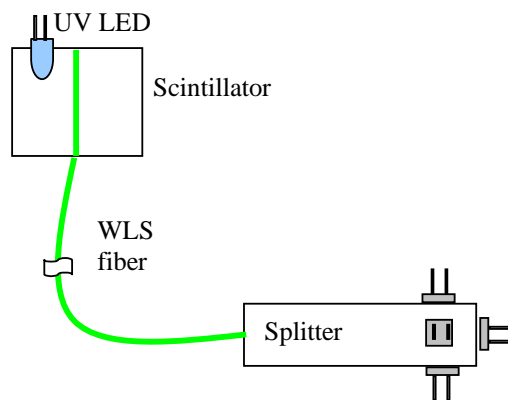


Fig. 2a.

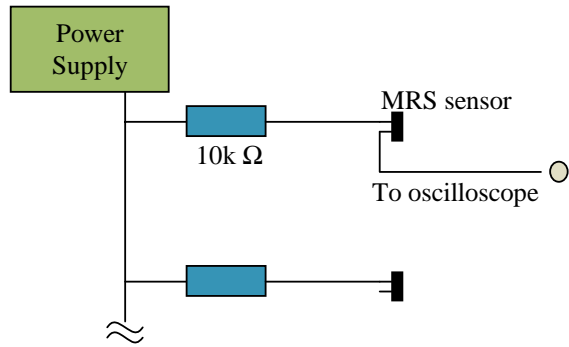


Fig. 2b.

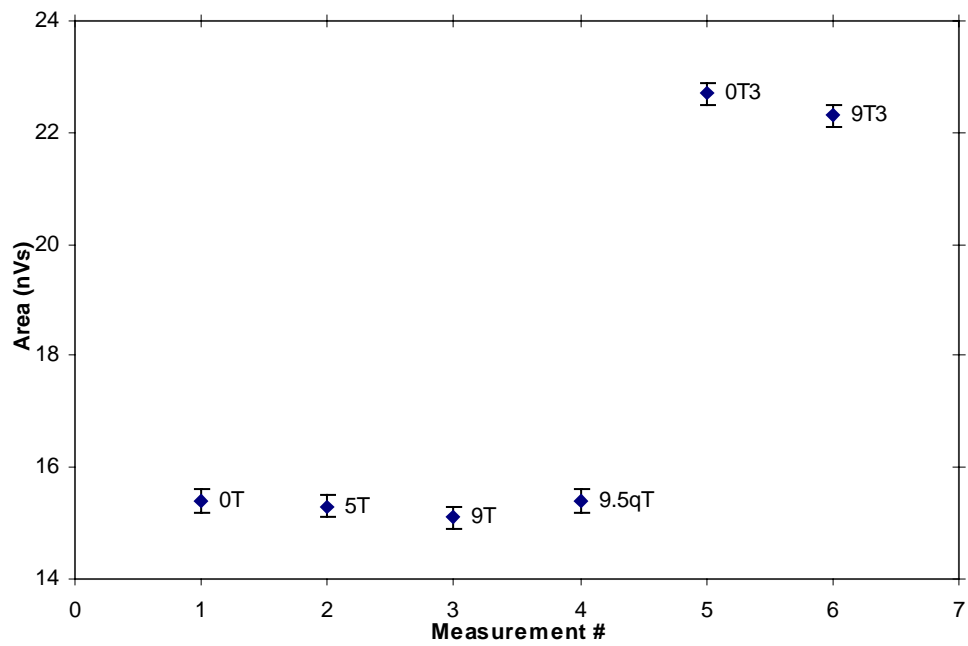


Fig. 3.

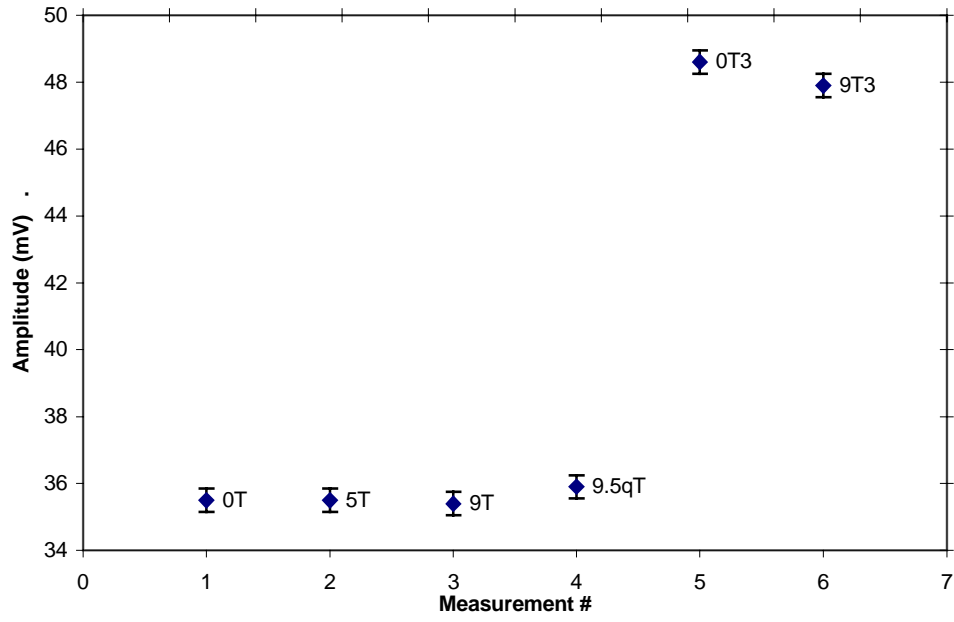


Fig. 4.

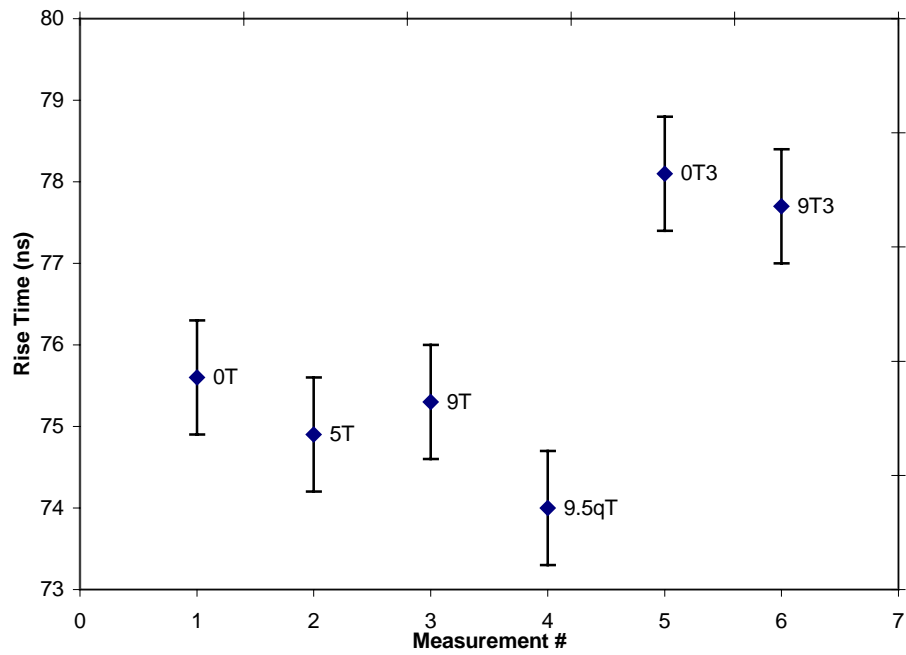


Fig. 5.